Evaluation of Crosslinking Conditions on the Properties of Chitosan Woven Meshes

Henrique Nunes Da Silva[a] ![ORCID], *Marcelo Paulo Tissiani[a], Matheus Ferreira de Souza[a]* ![ORCID],

Maria Eduarda Vasconcelos Barreto[a] ![ORCID], *Rossemberg Cardoso Barbosa[a], Marcus Vinícius Lia Fook[a*]*

[a]*Universidade Federal de Campina Grande, Departamento de Engenharia de Materiais, Programa de Pós-Graduação em Ciência e Engenharia de Materiais, 58429-900, Campina Grande, PB, Brasil.*

Crosslinking of chitosan (CS) woven meshes is reported in this study. CS filaments were obtained by wet spinning and hand-waved. The weft was coated with CS solutions (3 and 4% w/v) and crosslinked with sodium tripolyphosphate or genipin. CS filaments were free from superficial pores, and their mechanical properties were suitable for the weaving process. CS concentration in the coating, type, and the crosslinking time affected the mesh morphology obtained. Crosslinking by both agents was confirmed by spectroscopy, corroborating the reduction of the hydrophilicity of the crosslinked samples in the swelling and contact angle tests. Crosslinking conditions were effective in reducing the mechanical properties variation in the wet state, as well as regulating the degradation rate of the samples. Furthermore, it was observed that crosslinking did not significantly affect the cell viability of CS woven meshes, making them promising materials for application as stress material in a physiological environment.

Keywords: *Chitosan, filaments, weaving, woven mesh, crosslinking.*

1. Introduction

The medical textile industry has grown considerably, driving research interests for different solutions in the health field, such as infection control, dressings, wound care products, and medical devices. Thus, there is a significant increase in the development of new fibers and new technologies for manufacturing yarns and fabrics. Many modern medical textile products are made from fiber components based on synthetic polymer, including polylactic acid (PLA), polycaprolactone (PCL), and polypropylene (PP); and natural ones such as collagen, chitin, and chitosan (CS)[1-4].

Chitosan is a natural polysaccharide obtained by chemical or enzymatic deacetylation of chitin. Its chemical structure consists of glucosamine and N-acetyl glucosamine units linked by β- glycosidic bonds (1 → 4). When the degree of deacetylation of CS reaches about 50%, it becomes soluble in an aqueous acidic solution[5,6]. It has non-toxicity, biocompatibility, biodegradability, and hemostatic properties, and is easily processed when in weak acidic solutions, allowing the design of different configurations for the development of medical textile products[6-8], such as scaffolds[9,10], films[11-13], and filaments[14-16].

A common technique for developing CS filaments is wet spinning, which consists of extruding a polymeric solution into a non-solvent, promoting an acid-base neutralization[17,18]. These filaments can be processed to result in fibrous textile structures, including fabrics, meshes, braids, and non-wovens, which can have an architecture designed to meet specific requirements for applications in the biomedical field[19-21]. Neves et al.[21] developed a fiber-mesh scaffold based on CS/PCL blends for cartilage repair from fiber production via wet spinning. Kim et al.[22] produced fabric composites based on CS/hydroxyapatite (HAp) by wet spinning with potential properties for application in bone tissue engineering. Nowotny et al.[9], by the wet spinning of CS fibers, produced braided scaffolds, achieving a simple approach to design tendon analogs. Yu et al.[23] developed a warp-knitted mesh from CS filaments for stress application in hernia repair.

In a previous work by our research group[24], mono and multifilament CS woven meshes were developed. It was observed that the mechanical and morphological properties are modulable based on the configuration of the yarn used in weaving. The authors observed that after hydration, the tensile strength of the monofilament mesh was reduced by 46.8%, while the deformation was increased by 30 times compared to the dry state and its degradation was 80.3% in 5 weeks, suggesting potential applications in the biomedical field, as dressings, or controlled drug release systems.

Mechanical properties of CS-based materials are reduced in the wet state due to the high hydrophilicity and, consequently, the swelling behavior[14]. These characteristics can be regulated through crosslinking processes[25]. In this sense, the use of crosslinking agents such as sodium tripolyphosphate (TPP)[25-28] and genipin[29-31] is widely investigated. In addition, the adjustment of crosslinking process also promotes modulation of the degradation rate for specific applications[32-34].

To the best of our knowledge, the effects of crosslinking on the properties of CS woven meshes have not been investigated yet. In this sense, this work aims to develop crosslinked chitosan woven meshes, to evaluate the effect of crosslinking with TPP and genipin on their properties.

*e-mail: marcus.liafook@certbio.ufcg.edu.br

2. Experimental

2.1. Materials

Chitosan (medical degree) 96% deacetylated and molar weight of 310 KDa was produced by CERTBIO (Laboratory of Biomaterials Assessment and Development from Northeast). Phosphate buffer saline, lysozyme, Genipin, and sodium tripolyphosphate (TPP) were bought from Sigma Aldrich. Lactic acid and sodium hydroxide were acquired from Vetec.

2.2. Samples preparations

2.2.1. Filaments

CS filaments were produced according to the methodology reported by Silva et al.[35]. CS solution with 4% (m/v) was prepared by dissolution of the polysaccharide in lactic acidic solution (1% v/v) under mechanical agitation (400 rpm) for 2 hours at 25 ± 1 °C. Then the CS solution was centrifuged to remove air bubbles and extruded with an infusion pump (Pump 11 Pico Plus Elite, Harvard Apparatus) through a die (45 mL/h, 1 mm diameter outlet tip) immersed in a coagulation bath containing 1 M sodium hydroxide solution. The solidified filaments were submerged in the coagulation bath for 1 h. After total coagulation, the threads were washed in distilled water to pH 7 and dried in a kiln with forced air circulation at 40 °C for 24 h.

2.2.2. Woven meshes

CS threads were used in a handmade weaving process, aiming the obtention of woven mesh materials according to the methodology reported in our other work[24]. PET-G (glycol-modified poly (ethylene terephthalate) 3D-printed mold used for the weaving process is shown in Figure 1. The diameter and spacing between mold pins were 3 mm, and the edge was 6 mm (Figure 1b,c). After the weaving process, the CS woven meshes were impregnated with 5 mL of 3 and 4% CS solutions to keep the weft between the threads. The coated woven meshes were submerged in 1 M sodium hydroxide solution for 1 h to request the coating, then proceeded with washing for neutralization (pH 7) with distilled water and kiln drying (50 °C for 6 h). The CS solutions for the coating were prepared according to the methodology described above for the threads, varying only the CS concentration.

2.2.3. Crosslinked woven meshes

Coated dried CS woven meshes were crosslinked with 100 mL of aqueous solutions at 0.5% (m/v) for both crosslinking agents (genipin and sodium tripolyphosphate) at 15 and 30 minutes. Then, it was proceeded with washing with distilled water and kiln drying at 35 °C for 24 h. The solutions were prepared by adding the crosslinking agents to deionized water under magnetic stirring for 30 minutes. The samples were coded as shown in Table 1.

2.3. Characterizations

CS filaments, non-crosslinked woven meshes, and all crosslinked samples were characterized by optical microscopy (OM) and mechanical tensile test. Some crosslinked samples were evaluated by FT-IR spectroscopy, contact angle, *in vitro* biodegradation, swelling, and *in vitro* cytotoxicity tests.

Table 1. Coding of prepared samples.

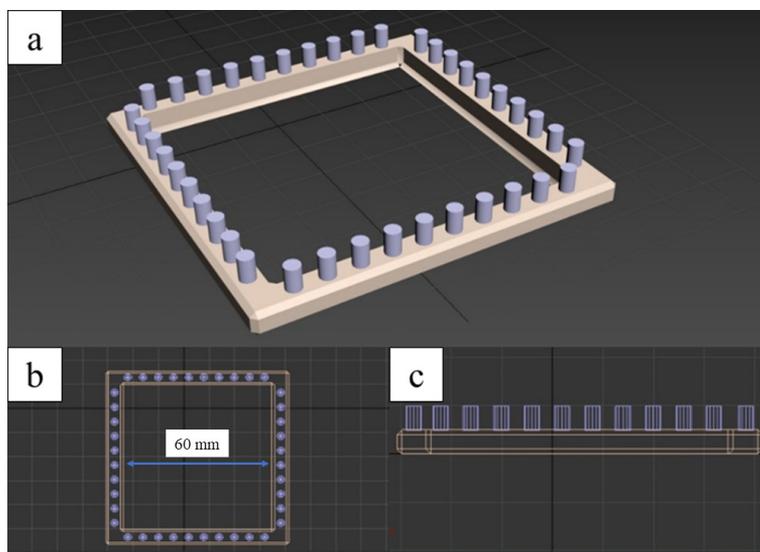| Woven mesh samples	CS coating concentration (%)	Crosslinking agent	Crosslinking Time (min)
3CS	3	-	-
3CST15	3	TPP	15
3CST30	3	TPP	30
3CSG15	3	Genipin	15
3CSG30	3	Genipin	30
4CS	4	-	-
4CST15	4	TPP	15
4CST30	4	TPP	30
4CSG15	4	Genipin	15
4CSG30	4	Genipin	30

Figure 1. Views of the mold made by 3D printing for weaving of the CS meshes.

An optical microscope (Hirox Digital Microscope, Kh 1,300 M, Tokyo, Japan) was used to obtain OM images of the CS filaments and woven meshes. The openings of the meshes were evaluated using ImageJ software.

Uniaxial tensile tests were used to characterize the mechanical properties of CS filaments (n = 10) and woven meshes (n = 5). Experiments were conducted on universal mechanical properties testing apparatus (Instron Model 6633), equipped with a load cell of 500 kN, at 24 ± 2 °C and relative humidity of $60\% \pm 2\%$. The traction velocity was 120 mm/min for filaments and 100 mm/min for woven meshes samples. The specimens were 100 mm for filaments and 60 mm x 10 mm. FT-IR analyzes were performed on a Perkin Elmer spectrophotometer Spectrum 400 (4000 – 650 cm^{-1}).

For contact angle tests, was used a goniometer developed by the Mechanical Engineering Academic Unit at UFCG (Federal University of Campina Grande). Deionized water was utilized as a contact liquid. Photographs were taken after 10 seconds of liquid contact with the sample surface (n = 5) and the measurements were performed with Angle Calculator software.

The swelling behavior of the CS woven meshes was evaluated after 24 h of contact with phosphate buffer solution (PBS, pH = 7.34) at 37 ± 0.5 °C, besides that, mechanical properties were too evaluated in the wet state, according to the conditions described above for uniaxial tensile tests. The samples were weighed (n = 5) in dry (W_d) and wet conditions (W_w) for swelling degree calculation according to Equation 1.

$$Swelling\ degree\ in\ 24\ h\ (\%) = \frac{W_w - W_d}{W_d} x100\% \tag{1}$$

Biodegradation of the CS woven meshes was evaluated through weight loss in phosphate buffer solution (pH = 7.34) at 37 ± 0.5 °C containing lysozyme at 1.5 µg/mL[24,36]. The samples were dried at 50 °C for 6 h, weighed (W_0), and conditioned at degradation medium. At each biodegradation period (1, 2, 3, 4, and 5 weeks), the CS woven meshes samples were taken from the solution, washed in distilled water, pre-dried with absorbent paper, and then weighed (W_t). The biodegradation results were obtained from Equation 2.

$$Weight\ loss\ (\%) = \frac{W_0 - W_t}{W_0} x100\% \tag{2}$$

In vitro cytotoxicity of the CS woven meshes was evaluated using MTT cell availability evaluation test according to ISO 10993 - 5: 2009, with direct contact between samples and L929 fibroblasts cells. The Grubbs test was performed for outliers. The calculation of the standard deviation was performed by Graph Pad Prism 6. The spectrophotometer used to read the viability of the cells was the Victor X3 device, Perkin Elmer, with the measurement wavelength at 570 nm and the reference wavelength at 650 nm.

3. Results and Discussions

3.1. CS filaments preparation

3.1.1. Morphology

Figure 2 presents OM images of CS filaments. A relatively smooth and compact cylindrical monofilament morphology is observed, without surface pores and an average diameter of 0.180 ± 0.013 mm (n = 5). This morphology provides a uniform distribution of stresses along the wire[37]. There is also the presence of longitudinal grooves, probably due to the outlet tip or orientation of the polymer chains of chitosan caused by the wet spinning process[38]. In the image of the cross-section of the filament, it is observed an almost circular geometry with a rough surface resulting from the fracture and the presence of pores inside the filament.

3.1.2. Mechanical properties

Table 2 shows the mechanical properties of CS filaments obtained by wet spinning. These properties are essential to determine the performance of the treads in the weaving process and, consequently, of the final product. The results obtained here were similar to those reported by Silva et al.[36,39] in his work with chitosan threads for application as surgical suture material.

Table 2. Mechanical properties of CS filament obtained by wet spinning.

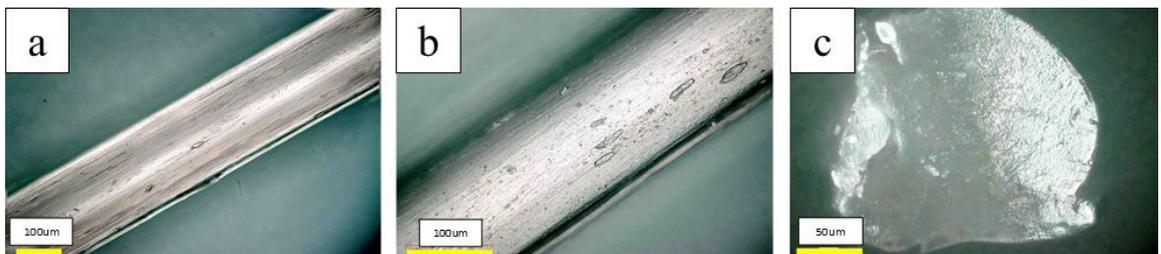|	
Maximum load (N)	6.2 ± 0.42
Tensile strength (MPa)	248 ± 12.61
Strain (%)	2.3 ± 0.18
Youngs Module (GPa)	29.1 ± 3.00

Figure 2. OM images of 4% CS filament obtained by wet spinning. Increases of a) 350x the longitudinal section, b) 700x the longitudinal section and c) 1050x the cross-section of the filament.

3.2. CS woven meshes preparation

Figures 3a and 3b show OM microscopy of the CS woven meshes coated with 3 and 4% CS solutions, respectively.

Uniform coatings throughout the length of the samples can be observed, showing that both CS solutions, 3 and 4%, were efficient in producing homogeneous coatings. It is also possible to observe marks on the coating at higher magnifications, probably due to the accumulation of solution near the wires. There is a typical morphology of woven structures in the 1/1 ratio (flat fabric)[40-42]. In addition to the appearance and uniformity of the coating, the openings of CS woven meshes were 7.5 ± 0.38 and 7.3 ± 0.55 mm² for meshes coated with the 3 and 4% CS solutions, respectively.

3.3. Crosslinked CS woven meshes preparation

3.3.1. Morphology

Figure 4 shows the CS woven meshes after crosslinking with different agents (Genipin and sodium tripolyphosphate) and times (15 and 30 minutes). Sodium tripolyphosphate crosslinked samples showed more uniform morphology than those crosslinked with Genipin, and only the 3CSG15 sample did not show retraction. The retraction and the increase in surface roughness are in agreement with that reported by Hillberg et al.[43] for materials crosslinked with genipin. Furthermore, it is notable that the genipin crosslinked samples were dark, in bluish-green tones, characteristic of this reagent[44].

In images magnified by OM, it is possible to observe that the samples obtained with 3% CS coating had fewer rough surfaces compared to those obtained with 4% CS coating, for both crosslinking agents, in particular for the longer crosslinking time (30 minutes). This is probably due to the high viscosity of the more concentrated chitosan solution, which prevented the formation of a more homogeneous film on the filaments[45].

3.3.2. Mechanical properties

Results of mechanical tests are present in Figure 5. It is possible to notice a growing tendency in the capacity of the woven meshes to support the load with the increase of the CS concentration in the coating. This effect is due to the greater entanglement of polymer chains when more materials are deposited on the filaments[46-48]. Crosslinked samples showed a drop of maximum load compared to those uncrosslinked. The strain and tensile strength of CS woven meshes decrease with crosslinking for all tested conditions due to the restriction of the polymeric chains by the introduction of crosslinks[48,49]. These results corroborate with the studies reported by Butler et al.[44], Hwang and Shin[47], Wyatt et al.[48], Mi et al.[50], and Cui et al.[51].

The samples 3CS, 3CST15, 3CST30, 3CSG15, 4CS, and 4CST30 were the ones that showed higher tensile strength in the dry state, and therefore were selected for the subsequent characterizations.

3.3.3. FT-IR spectroscopy

Analysis of CS woven meshes by FT-IR spectroscopy was performed to evaluate its crosslinking with TPP and genipin. FT-IR spectra are shown in Figure 6a. It is observed that there were interactions between CS and both crosslinking agents, evidenced by the intensity reduction of the hydroxyl and amine bands at 3330 cm⁻¹ and protonated amine in 1078 cm⁻¹, indicating a decrease in hydrogen bonds[52].

The peaks intensity reductions around 1577 and 1028 cm⁻¹ are due to the bonds formed between amino groups of CS and carboxymethyl units of genipin, forming
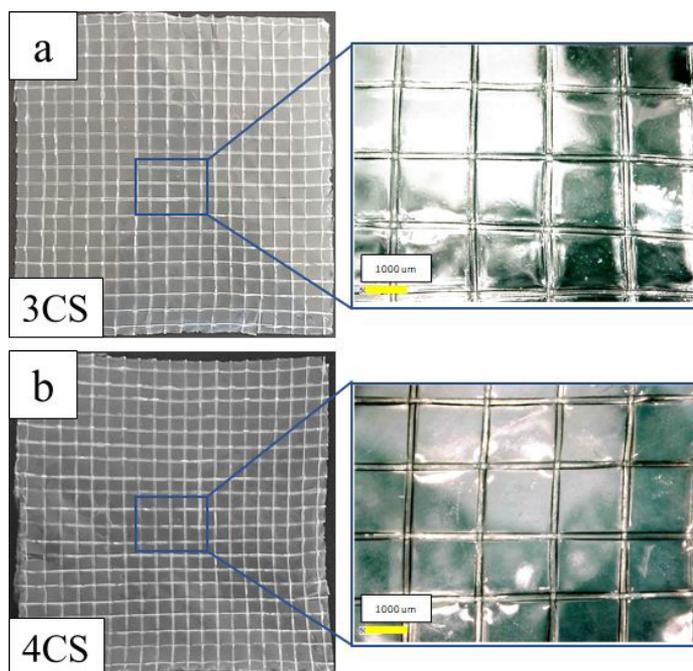

Figure 3. OM images of CS woven meshes. a) coated with 3% CS solution, b) coated with 4% CS solution.
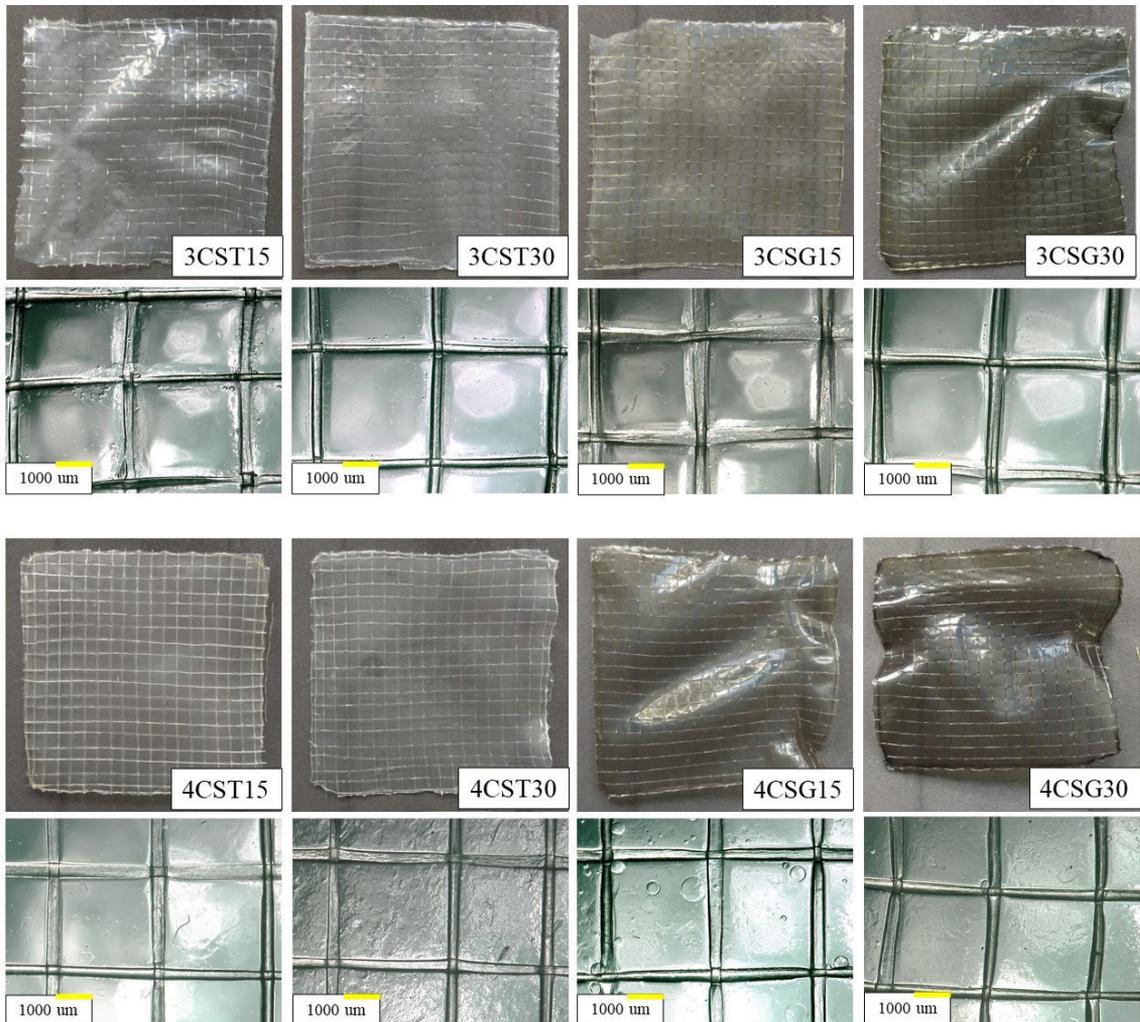
Figure 4. OM images of CS woven meshes crosslinked with TPP and genipin at different times.

secondary amide[53-55]. The effect occurs similarly for the bands located between 3361.42 and 2876.76 cm^{-1} since the bonds formed by hydroxyls are also preferential points of chemical crosslinking[56].

The spectra of the samples with and without crosslinking showed the characteristic absorption bands of CS. At 3330 cm^{-1} related to the superposition of the elongation vibrations of the amine and hydroxyl group, peaks around 1575 cm^{-1} associated with the protonated amino group, and in 1078 and 1025 cm^{-1} resulting from the elongation of the C-N and C-O bonds, respectively[51].

Through the detail presented in Figure 6b, the reduction in band intensity at 1575 cm^{-1} can be interpreted as the formation of secondary amide after the protonated amine is consumed by reaction with the genipin ester groups[44]. The increase in the intensity of the vibration band of the C-N bond at 1070 cm^{-1} suggests the formation of crosslinked compounds[51].

In Figure 6c, the complexation of chitosan with TPP molecules is suggested by the higher peak intensities at 1150 cm^{-1} attributed to the P-O bond and at 892 cm^{-1} related to the asymmetric stretching of the P-O-P bond[57].

3.3.4. Swelling behavior

The Swelling degree (%) of CS woven meshes are shown in Figure 7. The uncrosslinked samples exhibited the highest swelling degrees, followed by those crosslinked with sodium tripolyphosphate and genipin, respectively. On the other hand, the sample 3CS presented the lowest swelling degree, probably due to its higher degree of crosslinking, as suggested by the FT-IR results.

CS-based materials swell through hydrophilic interactions (hydrogen bridges) between water molecules and the chitosan amine and hydroxyl groups. As the crosslinking degree increases, the functional groups available for interactions decreases. Furthermore, the crosslinks limit the expansion of the polymeric network, hindering the absorption of fluids[58-60]. Thus, the amount of fluid absorbed (degree of swelling) must be inversely related to the crosslinking degree of the samples, as reported by Klein et al.[61].

The effect of swelling on the mechanical properties of CS woven meshes was also investigated. The results are shown in Table 3. After swelling, the uncrosslinked
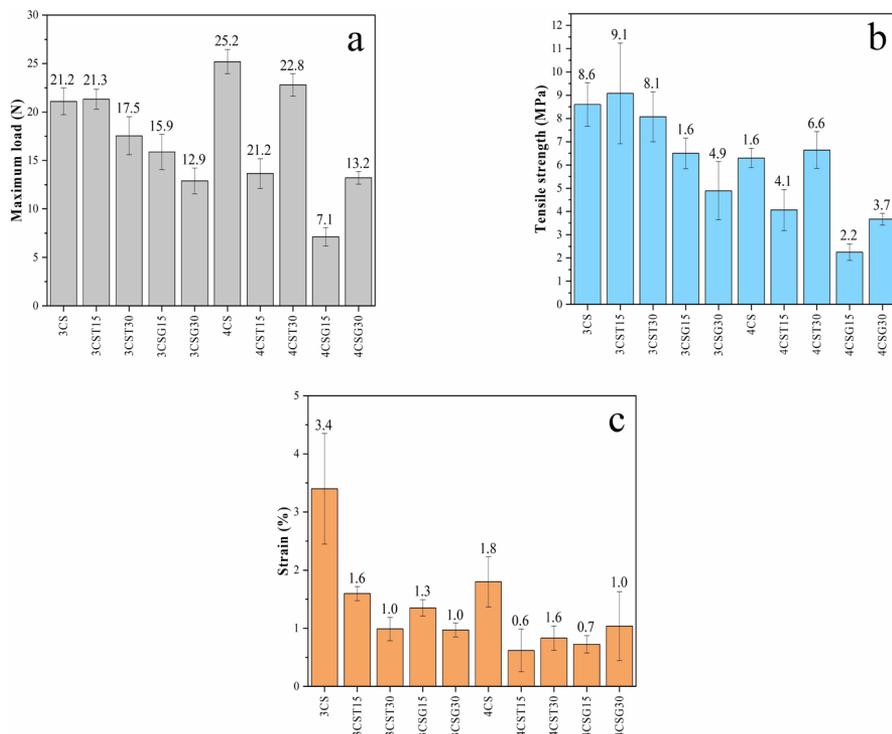
Figure 5. Mechanical properties of crosslinked and uncrosslinked CS woven meshes a) maximum load; b) tensile strength and c) strain.
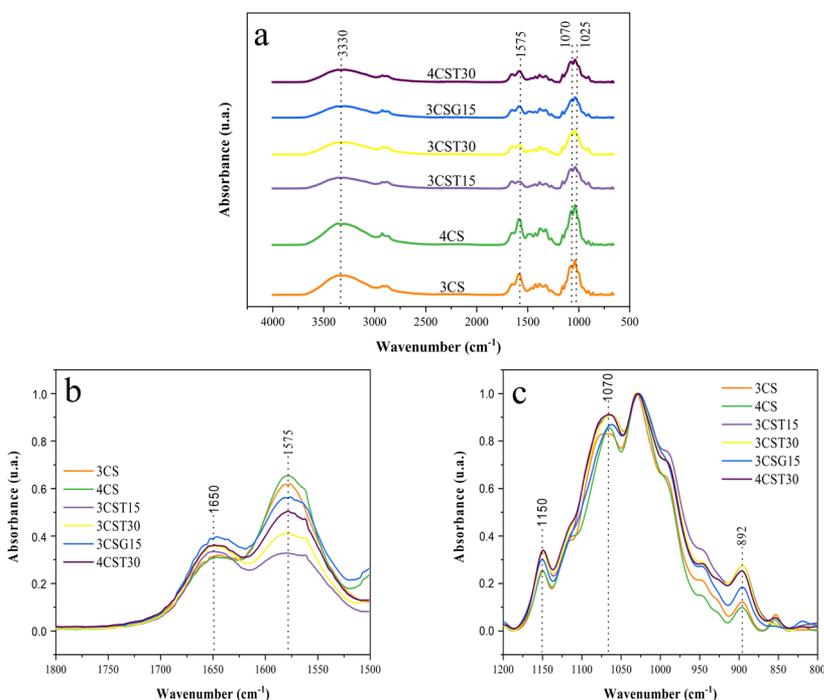

Figure 6. FT-IR spectra of crosslinked and uncrosslinked CS woven meshes a) from 4000 to 650 cm^{-1}; b) from 1800 to 1500 cm^{-1} and c) from 1200 to 800 cm^{-1}.

samples presented the lowest maximum loads, which shows the improvement of this property by the crosslinking process. Among the crosslinked samples, those that received the sodium tripolyphosphate treatment performed better

than those treated with genipin. The swelling promoted a reduction in tensile strength and an expressive gain in deformation of all samples. However, in the wet state, the sample crosslinked with genipin (3CSG15) showed greater

Table 3. Mechanical properties of the CS woven meshes crosslinked with TPP and genipin at different times in the dry and wet state.

Sample	State	Maximum load (N)	Tensile strength (MPa)	Strain (%)
3CS	Dry	21.1 ± 1.38	8.6 ± 0.94	3.4 ± 0.95
	Wet	8.1 ± 0.73	4.1 ± 0.68	32.2 ± 0.38
4CS	Dry	25.2 ± 1.25	6.3 ± 0.41	1.8 ± 0.43
	Wet	9.2 ± 0.16	4.2 ± 0.71	29.3 ± 0.73
3CST15	Dry	21.3 ± 1.04	9.1 ± 2.16	1.6 ± 0.12
	Wet	16.3 ± 0.06	3.9 ± 0.03	16.1 ± 1.6
3CST30	Dry	17.5 ± 1.96	8.1 ± 1.07	1.0 ± 0.20
	Wet	12.8 ± 0.16	3.6 ± 0.06	26.2 ± 2.71
3CSG15	Dry	15.9 ± 1.82	6.5 ± 0.66	1.3 ± 0.14
	Wet	9.4 ± 0.82	4.4 ± 0.06	6.2 ± 0.96
4CST30	Dry	22.8 ± 1.14	6.6 ± 0.79	0.8 ± 0.21
	Wet	15.3 ± 0.25	3.1 ± 0.03	22.7 ± 1.5

Mean ± Standard deviation.

tensile strength than the sample without crosslinking (3CS) and lower deformation capacity than the sodium tripolyphosphate crosslinked samples.

Table 4 presents the variations (%) of the mechanical properties when going from the dry to the wet state. Crosslinking with sodium tripolyphosphate and genipin reduced the decrease in maximum load by swelling the samples. Variations in tensile strength and deformation appear to have been unaffected by crosslinking.

According to Wu et al.[62], the wet mechanical behavior of biomaterials is more important than the dry state. The water molecules absorbed by the samples interfere with the intermolecular hydrogen bonds of the CS chains. The intermolecular interactions are reduced, facilitating the sliding of the chains and improving the polymers ability to deform[63-65]. This behavior in the wet state is reported in the literature by other authors[66-68].

3.3.5. Contact angle

Figure 8 shows the result of the contact angle test. According to Sengupta and Pittman[69], the wettability of a solid surface decreases as the contact angle with the water drop increases. Angles smaller than 90° mean that the liquid tends to wet the sample, therefore, the surface is hydrophilic. In this case, the investigated samples have a hydrophilic character, as they presented contact angles below 90°.
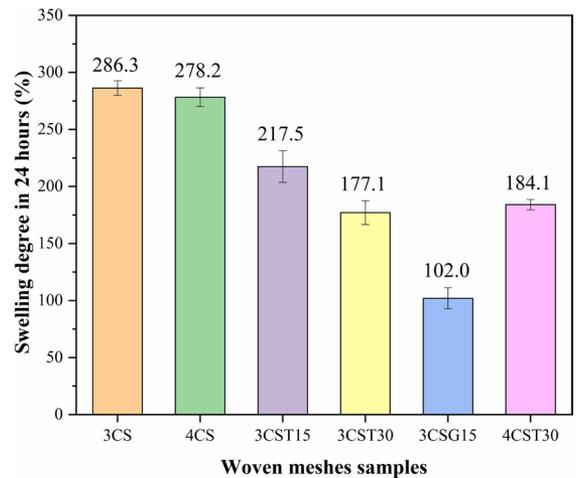
Uncrosslinked samples had the smallest contact angles. That is, they were more hydrophilic than crosslinked samples. There was a decrease in the availability of polar groups in the crosslinked samples, decreasing their polarity and wettability. These results are in accord with those reported by Jin et al.[70], Karbasi et al.[71], and Tabriz et al.[72].

3.3.6. Biodegradation

The enzymatic biodegradation profiles of the samples with and without crosslinking are shown in Figure 9. Up to two weeks, all samples showed only mass fluctuations related to swelling and interactions between the degradation fluid and the amorphous and crystalline regions of the samples[24]. After two weeks, the mass loss starts for most of them. The 3CS and 3CST15 samples had the highest biodegradation rates, followed by the 3CST30 one. The 3CSG15 sample showed a lower degradation rate, with practically constant

Table 4. Variation of the mechanical properties when going from dry to a hydrated state.

Sample	Maximum load	Tensile strength	Strain
3CS	-62	-52	847
4CS	-96	-33	1528
3CST15	-23	-57	906
3CST30	-27	-56	2520
3CSG15	-41	-32	377
4CST30	-33	-53	2738

Figure 7. Swelling degree of CS woven meshes crosslinked with TPP and genipin at different times.

mass for 4 weeks, showing that crosslinking with genipin was efficient in delaying the biodegradation process of the CS woven meshes.

3.3.7. In vitro cytotoxicity

Figure 10 shows the cell viability of the uncrosslinked and crosslinked CS woven meshes. Following ISO 10993-5, all samples demonstrated to be biocompatible, with cell viability higher than 70%. The biocompatibility of
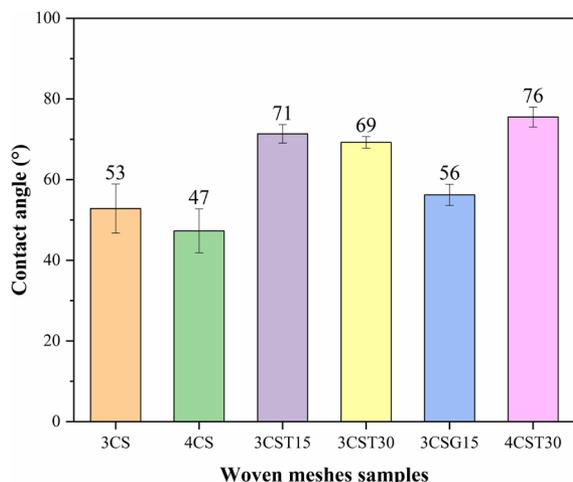
Figure 8. Contact angle of the CS woven meshes crosslinked with TPP and genipin at different times.
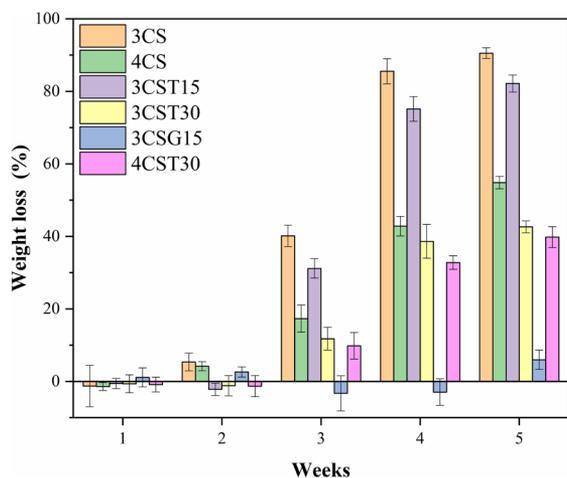

Figure 9. Mass variation of the CS woven meshes crosslinked with TPP and genipin at different times.
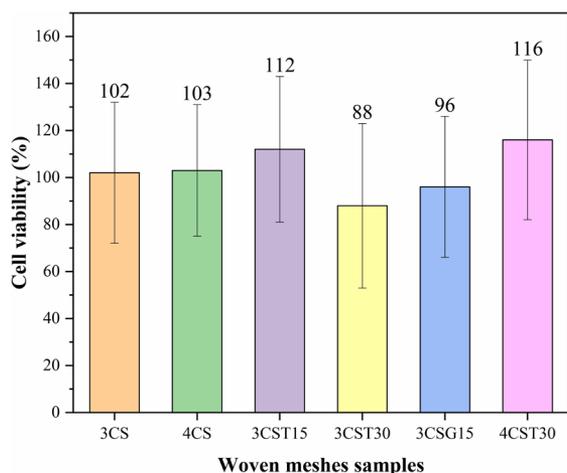

Figure 10. Cell viability of the CS woven meshes crosslinked with TPP and genipin at different times.

chitosan-based materials is widely reported in the literature. Several structures were evaluated, including electrospun nanofibers[73,74], nanoparticles[75,76], microspheres[77], and porous scaffolds[78]. The crosslinking process did not significantly affect the biocompatibility of the samples, corroborating the works reported by Mi et al.[79], Bi et al.[80], Zhang et al.[33], and Dimida et al.[32].

4. Conclusions

Crosslinked CS woven meshes were obtained from the manual weaving of CS filaments. The crosslinking conditions affected the morphology and mechanical properties of the woven meshes. The effective crosslinking by genipin and TPP was proven by spectroscopy. Crosslinking increased the mechanical stability in the wet state and promoted the modulation of swelling and biodegradation. In addition, it did not significantly affect the hydrophilicity and biocompatibility of CS woven meshes. Thus, the materials developed in this work are promising for stress application in a physiological environment.

5. Acknowledgments

6. References

1. Petrulyte S, Petrulis D. Modern textiles and biomaterials for healthcare. In Bartels VT, editor. Handbook of medical textiles. Oxford: Woodhead Publishing; 2011. p. 1-35.
2. Rohani Shirvan A, Nouri A. Medical textiles. In Ul-Islam S, Butola BS, editors. Advances in functional and protective textiles. Duxford: Woodhead Publishing; 2020. p. 291-333.
3. Gorgieva S, Zemljić LF, Strnad S, Kokol V. Textile-based biomaterials for surgical applications. In: Thomas S, Balakrishnan P, Sreekala MS, editors. Fundamental biomaterials: polymers. Duxford: Woodhead Publishing; 2018. p. 179-215.
4. Kennedy JF, Knill CJ. Biomaterials utilised in medical textiles: an overview. In: Anand SC, editor. Medical textiles and biomaterials for healthcare. Boca Raton: Taylor & Francis; 2006. p. 3-22.
5. Chang KLB, Tsai G, Lee J, Fu W. Heterogeneous N-deacetylation of chitin in alkaline solution. Carbohydr Res. 1997;303(3):327-32.
6. Rinaudo M. Chitin and chitosan: properties and applications. Prog Polym Sci. 2006;31(7):603-32.
7. Leceta I, Guerrero P, De La Caba K. Functional properties of chitosan-based films. Carbohydr Polym. 2013;93(1):339-46.
8. Jennings JA, Bumgardner JD. Chitosan based biomaterials - Volume 1: Fundamentals. Amsterdam: Woodhead Publishing; 2016.
9. Nowotny J, Aibibu D, Farack J, Nimtschke U, Hild M, Gelinsky M, et al. Novel fiber-based pure chitosan scaffold for tendon augmentation: biomechanical and cell biological evaluation. J Biomater Sci Polym Ed. 2016;27(10):917-36.
10. Sadeghianmaryan A, Naghieh S, Sardroud HA, Yazdanpanah Z, Soltani YA, Sernaglia J, et al. Extrusion-based printing of chitosan scaffolds and their in vitro characterization for cartilage tissue engineering. Int J Biol Macromol. 2020;164:3179-92.
11. Colobatiu L, Gavan A, Potarniche A-V, Rus V, Diaconeasa Z, Mocan A, et al. Evaluation of bioactive compounds-loaded

chitosan films as a novel and potential diabetic wound dressing material. React Funct Polym. 2019;145:104369.

12. Brás T, Rosa D, Gonçalves AC, Gomes AC, Alves VD, Crespo JG, et al. Development of bioactive films based on chitosan and Cynara cardunculus leaves extracts for wound dressings. Int J Biol Macromol. 2020;163:1707-18.

13. Zarandona I, Barba C, Guerrero P, de la Caba K, Maté J. Development of chitosan films containing β-cyclodextrin inclusion complex for controlled release of bioactives. Food Hydrocoll. 2020;104:105720.

14. Yudin VE, Dobrovolskaya IP, Neelov IM, Dresvyanina EN, Popryadukhin PV, Ivankova EM, et al. Wet spinning of fibers made of chitosan and chitin nanofibrils. Carbohydr Polym. 2014;108:176-82.

15. Sibaja B, Culbertson E, Marshall P, Boy R, Broughton RM, Solano AA, et al. Preparation of alginate–chitosan fibers with potential biomedical applications. Carbohydr Polym. 2015;134:598-608.

16. Mohammadkhani G, Kumar Ramamoorthy S, Adolfsson KH, Mahboubi A, Hakkarainen M, Zamani A. New solvent and coagulating agent for development of chitosan fibers by wet spinning. Polymers. 2021;13(13):2121.

17. Kumar MNVR. Chitin and chitosan fibres: a review. Bull Mater Sci. 1999;22(5):905-15.

18. Zhang D. Advances in filament yarn spinning of textiles and polymers. Oxford: Elsevier; 2014.

19. Sumanasinghe R, King M. The challenge of tissue engineering. J Text Apparel Technol Manage. 2003;3:1-13.

20. Chang C, Ginn B, Livingston NK, Yao Z, Slavin B, King MW, et al. Medical fibers and biotextiles. In: Wagner W, Sakiyama-Elbert S, Zhang G, Yaszemski MJ, editors. Biomaterials Science. 4th ed. Amsterdam: Academic Press; 2020. p. 575-600.

21. Neves SC, Teixeira LSM, Moroni L, Reis RL, Van Blitterswijk CA, Alves NM, et al. Chitosan/Poly (ε-caprolactone) blend scaffolds for cartilage repair. Biomaterials. 2011;32(4):1068-79.

22. Kim BS, Kim JS, Chung YS, Sin YW, Ryu KH, Lee J, et al. Growth and osteogenic differentiation of alveolar human bone marrow-derived mesenchymal stem cells on chitosan/hydroxyapatite composite fabric. J Biomed Mater Res A. 2013;101(6):1550-8.

23. Yu S, Ma P, Cong H, Jiang G. Preparation and performances of warp-knitted hernia repair mesh fabricated with chitosan fiber. Polymers (Basel). 2019;11(4):595.

24. Silva HN, Silva MC, Santos FSF, Silva JAC Jr, Barbosa RC, Fook MVL. Chitosan woven meshes: influence of threads configuration on mechanical, morphological, and physiological properties. Polymers (Basel). 2021;13(1):47.

25. Wahba MI. Enhancement of the mechanical properties of chitosan. J Biomater Sci Polym Ed. 2020;31(3):350-75.

26. Lusiana RA, Protoningtyas WP, Wijaya AR, Siswanta D, Santosa SJ. Chitosan-Tripoly Phosphate (CS-TPP) synthesis through cross-linking process: the effect of concentration towards membrane mechanical characteristic and urea permeation. Orient J Chem. 2017;33(6):2913-9.

27. Wahba MI. Porous chitosan beads of superior mechanical properties for the covalent immobilization of enzymes. Int J Biol Macromol. 2017;105:894-904.

28. Silvestro I, Francolini I, Di Lisio V, Martinelli A, Pietrelli L, Scotto d'Abusco A, et al. Preparation and characterization of TPP-chitosan crosslinked scaffolds for tissue engineering. Materials (Basel). 2020;13(16):3577.

29. Li Y, Cheng C, Wang N, Tan H, Tsai Y, Hsiao C, et al. Characterization of the modified chitosan membrane cross-linked with genipin for the cultured corneal epithelial cells. Colloids Surf B Biointerfaces. 2015;126:237-44.

30. Kildeeva N, Chalykh A, Belokon M, Petrova T, Matveev V, Svidchenko E, et al. Influence of genipin crosslinking on the properties of chitosan-based films. Polymers. 2020;12(5):1086.

31. Perez-Puyana V, Rubio-Valle J, Jiménez-Rosado M, Guerrero A, Romero A. Chitosan as a potential alternative to collagen for the development of genipin-crosslinked scaffolds. React Funct Polym. 2020;146:104414.

32. Dimida S, Barca A, Cancelli N, De Benedictis V, Raucci MG, Demitri C. Effects of genipin concentration on cross-linked chitosan scaffolds for bone tissue engineering: structural characterization and evidence of biocompatibility features. Int J Polym Sci. 2017;2017:1-8.

33. Zhang W, Ren G, Xu H, Zhang J, Liu H, Mu S, et al. Genipin cross-linked chitosan hydrogel for the controlled release of tetracycline with controlled release property, lower cytotoxicity, and long-term bioactivity. J Polym Res. 2016;23(8):1-9.

34. Zhang Y, Wang QS, Yan K, Qi Y, Wang GF, Cui YL. Preparation, characterization, and evaluation of genipin crosslinked chitosan/gelatin three-dimensional scaffolds for liver tissue engineering applications. J Biomed Mater Res A. 2016;104(8):1863-70.

35. Silva MC, Silva HN, Cruz RCAL, Sagoe Amoah SK, Silva SML, Lia Fook MV. N-Acetyl-D-Glucosamine-Loaded chitosan filaments biodegradable and biocompatible for use as absorbable surgical suture materials. Materials (Basel). 2019;12(11):1807.

36. Silva MC, Silva HN, Holanda SA, Silva ARO, Fook MVL. Biodegradable polymeric wires: monofilament and multifilament. Mater Res Innov. 2019;24(3):166-70.

37. Barros M, Gorgal R, Machado AP, Correia A, Montenegro N. Princípios básicos em cirurgia: fios de sutura. Acta Med Port. 2011;24(S4):1051-6.

38. Dresvyanina E, Dobrovol'skaya IP, Popryadukhin PV, Yudin VE, Ivan'kova EM, Elokhovskii VY, et al. Influence of spinning conditions on properties of chitosan fibers. Fibre Chem. 2013;44(5):280-3.

39. Silva MC, Leal RDCA, Silva HN, Fook MVL. Biodegradable suture threads as controlled drug delivery systems. Mater Res Innov. 2019;24(3):161-5.

40. Tamayol A, Akbari M, Annabi N, Paul A, Khademhosseini A, Juncker D. Fiber-based tissue engineering: progress, challenges, and opportunities. Biotechnol Adv. 2013;31(5):669-87.

41. King MW, Gupta BS, Guidoin R. Biotextiles as medical implants. Cambridge: Elsevier; 2013.

42. Gupta B, Edwards J. Textile materials and structures for topical management of wounds. In: Rajendran S, editor. Advanced textiles for wound care, Duxford: Elsevier; 2019. p. 55-104.

43. Hillberg AL, Holmes CA, Tabrizian M. Effect of genipin cross-linking on the cellular adhesion properties of layer-by-layer assembled polyelectrolyte films. Biomaterials. 2009;30(27):4463-70.

44. Butler MF, Ng YF, Pudney PD. Mechanism and kinetics of the crosslinking reaction between biopolymers containing primary amine groups and genipin. J Polym Sci A Polym Chem. 2003;41(24):3941-53.

45. Aryaei A, Jayatissa AH, Jayasuriya AC. Nano and micro mechanical properties of uncross-linked and cross-linked chitosan films. J Mech Behav Biomed Mater. 2012;5(1):82-9.

46. Mucha M. Rheological characteristics of semi-dilute chitosan solutions. Macromol Chem Phys. 1997;198(2):471-84.

47. Hwang J, Shin H. Rheological properties of chitosan solutions. Korea-Australia Rheol J. 2000;12(4):175-9.

48. Wyatt NB, Gunther CM, Liberatore MW. Increasing viscosity in entangled polyelectrolyte solutions by the addition of salt. Polymer (Guildf). 2011;52(11):2437-44.

49. Chen M, Liu C, Tsai H, Lai W, Chang Y, Sung H. Mechanical properties, drug eluting characteristics and in vivo performance of a genipin-crosslinked chitosan polymeric stent. Biomaterials. 2009;30(29):5560-71.

50. Mi FL, Sung HW, Shyu SS. Synthesis and characterization of a novel chitosan-based network prepared using naturally occurring crosslinker. J Polym Sci A Polym Chem. 2000;38(15):2804-14.

51. Cui L, Jia J, Guo Y, Liu Y, Zhu P. Preparation and characterization of IPN hydrogels composed of chitosan and gelatin cross-linked by genipin. Carbohydr Polym. 2014;99:31-8.

52. Darbasizadeh B, Motasadizadeh H, Foroughi-Nia B, Farhadnejad H. Tripolyphosphate-crosslinked chitosan/poly (ethylene oxide) electrospun nanofibrous mats as a floating gastro-retentive delivery system for ranitidine hydrochloride. J Pharm Biomed Anal. 2018;153:63-75.

53. Chang K-C, Lin D-J, Wu Y, Chang C, Chen C, Ko C, et al. Characterization of genipin-crosslinked gelatin/hyaluronic acid-based hydrogel membranes and loaded with hinokitiol: in vitro evaluation of antibacterial activity and biocompatibility. Mater Sci Eng C. 2019;105:110074.

54. Shankar KG, Gostynska N, Montesi M, Panseri S, Sprio S, Kon E, et al. Investigation of different cross-linking approaches on 3D gelatin scaffolds for tissue engineering application: A comparative analysis. Int J Biol Macromol. 2017;95:1199-209.

55. Daniel-da-Silva AL, Salgueiro AM, Trindade T. Effects of Au nanoparticles on thermoresponsive genipin-crosslinked gelatin hydrogels. Gold Bull. 2013;46(1):25-33.

56. Wang L, Wang Y, Qu J, Hu Y, You R, Li M. The cytocompatibility of genipin-crosslinked silk fibroin films. J Biomater Nanobiotechnol. 2013;4(3):213-21.

57. Martins AF, Oliveira DM, Pereira AGB, Rubira AF, Muniz EC. Chitosan/TPP microparticles obtained by microemulsion method applied in controlled release of heparin. Int J Biol Macromol. 2012;51(5):1127-33.

58. Yao KD, Liu J, Cheng GX, Zhao RZ, Wang WH, Wei L. The dynamic swelling behaviour of chitosan-based hydrogels. Polym Int. 1998;45(2):191-4.

59. Gonçalves VL, Laranjeira M, Fávere VT, Pedrosa RC. Effect of crosslinking agents on chitosan microspheres in controlled release of diclofenac sodium. Polímeros. 2005;15(1):6-12.

60. Yodkhum K, Phaechamud T. Hydrophobic chitosan sponges modified by aluminum monostearate and dehydrothermal treatment as sustained drug delivery system. Mater Sci Eng C. 2014;42:715-25.

61. Klein MP, Hackenhaar CR, Lorenzoni AS, Rodrigues RC, Costa TM, Ninow JL, et al. Chitosan crosslinked with genipin as support matrix for application in food process: support characterization and β-d-galactosidase immobilization. Carbohydr Polym. 2016;137:184-90.

62. Wu T, Farnood R, OKelly K, Chen B. Mechanical behavior of transparent nanofibrillar cellulose–chitosan nanocomposite films in dry and wet conditions. J Mech Behav Biomed Mater. 2014;32:279-86.

63. Remuñán-López C, Bodmeier R. Mechanical, water uptake and permeability properties of crosslinked chitosan glutamate and alginate films. J Control Release. 1997;44(2-3):215-25.

64. Blasi PSSD, Souza FS, DeLuca PP. Plasticizing effect of water on poly (lactide-co-glycolide). J Control Release. 2005;108(1):1-9.

65. Alamri H, Low IM. Effect of water absorption on the mechanical properties of nano-filler reinforced epoxy nanocomposites. Mater Des. 2012;42:214-22.

66. Li J, Chen Y, Yin Y, Yao F, Yao K. Modulation of nano-hydroxyapatite size via formation on chitosan–gelatin network film in situ. Biomaterials. 2007;28(5):781-90.

67. Wang X, Li Q, Hu X, Ma L, You C, Zheng Y, et al. Fabrication and characterization of poly (l-lactide-co-glycolide) knitted mesh-reinforced collagen–chitosan hybrid scaffolds for dermal tissue engineering. J Mech Behav Biomed Mater. 2012;8:204-15.

68. Oh DX, Hwang DS. A biomimetic chitosan composite with improved mechanical properties in wet conditions. Biotechnol Prog. 2013;29(2):505-12.

69. Sengupta A, Pittman R. Application of membrane contactors as mass transfer devices. In: Hand book of membrane separations: chemical, pharmaceutical, food biotechnological application. New York: CRC Presss; 2008. p. 7-24.

70. Jin J, Song M, Hourston D. Novel chitosan-based films cross-linked by genipin with improved physical properties. Biomacromolecules. 2004;5(1):162-8.

71. Karbasi S, Khorasani SN, Ebrahimi S, Khalili S, Fekrat F, Sadeghi D. Preparation and characterization of poly (hydroxy butyrate)/chitosan blend scaffolds for tissue engineering applications. Adv Biomed Res. 2016;5(1):177.

72. Tabriz A, Alvi MAUR, Niazi MBK, Batool M, Bhatti MF, Khan AL, et al. Quaternized trimethyl functionalized chitosan based antifungal membranes for drinking water treatment. Carbohydr Polym. 2019;207:17-25.

73. Vulcani VAS, Bizarria MTM, d'Ávila MA, Mei LHI, Bernal C, Perussi J. Cytotoxicity tests for nanostructured chitosan/ PEO membranes using the agar diffusion method. Mater Res. 2012;15(2):213-7.

74. Zhao R, Li X, Sun B, Zhang Y, Zhang D, Tang Z, et al. Electrospun chitosan/sericin composite nanofibers with antibacterial property as potential wound dressings. Int J Biol Macromol. 2014;68:92-7.

75. Mansouri S, Lavigne P, Corsi K, Benderdour M, Beaumont E, Fernandes JC. Chitosan-DNA nanoparticles as non-viral vectors in gene therapy: strategies to improve transfection efficacy. Eur J Pharm Biopharm. 2004;57(1):1-8.

76. Rejinold NS, Muthunarayanan M, Muthuchelian K, Chennazhi K, Nair SV, Jayakumar R. Saponin-loaded chitosan nanoparticles and their cytotoxicity to cancer cell lines in vitro. Carbohydr Polym. 2011;84(1):407-16.

77. He Q, Ao Q, Wang A, Gong Y, Zhao N, Zhang X. In vitro cytotoxicity and protein drug release properties of chitosan/ heparin microspheres. Tsinghua Sci Technol. 2007;12(4):361-5.

78. Xu Y, Han J, Chai Y, Yuan S, Lin H, Zhang X. Development of porous chitosan/tripolyphosphate scaffolds with tunable uncross-linking primary amine content for bone tissue engineerin. Mater Sci Eng C. 2018;85:182-90.

79. Mi F, Tan Y, Liang H, Huang R, Sung H. In vitro evaluation of a chitosan membrane cross-linked with genipin. J Biomater Sci Polym Ed. 2001;12(8):835-50.

80. Bi L, Cao Z, Hu Y, Song Y, Yu L, Yang B, et al. Effects of different cross-linking conditions on the properties of genipin-cross-linked chitosan/collagen scaffolds for cartilage tissue engineering. J Mater Sci Mater Med. 2011;22(1):51-62.